G&G 2011

EXPLORING THE ORIGIN AND NATURE OF LUMINESCENT REGIONS IN CVD SYNTHETIC DIAMOND

Bert Willems, Alexandre Tallaire, and Julien Barjon

In the DiamondView instrument, blue to blue-green luminescent zones may be seen in CVD synthetic diamond when the growth run has been interrupted and resumed, a well-known practice in the production of gem-quality CVD synthetics. DiamondView, photoluminescence (PL), and cathodoluminescence (CL) imaging were applied to study the origin and nature of these luminescent regions in two samples of high-purity single-crystal CVD synthetic diamond. DiamondView and PL measurements showed a correlation with silicon-related centers. In addition, CL analysis confirmed the presence of boron. Both silicon and boron showed preferential incorporation at the interface between CVD layers, where a higher uptake of impurities lead to the observed luminescence. Although the growth interruptions cannot be detected with the naked eye, the growth history can be determined accurately using luminescence imaging and spectroscopy techniques.

Luminescence spectroscopy and imaging are important techniques for characterizing optical defects in diamond. The luminescence characteristics of diamond have been studied extensively and have provided insight into associated optical defect centers (see, e.g., Walker, 1979; Collins, 1992).

The Laboratoire des Sciences des Procédés et des Matériaux (LSPM; formerly known as Laboratoire d'Ingénierie des Matériaux et des Hautes Pressions, LIMHP) near Paris grows high-purity, unintentionally doped single-crystal chemical vapor deposition (CVD) synthetic diamond for high-power electronic devices (Kone et al., 2010). As part of the fabrication process for such applications, several active layers may be grown in different CVD reactors (Denisenko and Kohn, 2005), which requires that the growth run be interrupted and resumed in cycles. Although the CVD synthetic diamond samples studied here were thin plates rather than faceted gems, the same approach is applicable to the production of gem-quality CVD synthetic diamonds (figure 1), as it enables the growth of thick single crystals in three dimensions (Ho et al., 2006) and offers a method to control the bulk crystalline quality (Friel et al., 2009). The present study focuses on the luminescence generated by optical defect centers occurring in the process of these growth interruptions and resumptions (with pre- or intermediate etching steps). As such, gemologists can acquire in-depth information about the origin and growth history of these synthetic diamonds, which is crucial in differentiating them from natural material.

MATERIALS AND METHODS

The two synthetic diamond samples investigated here were grown at LSPM-CNRS using the plasma-assisted CVD method (Achard et al., 2005). Sample A was synthesized in a microwave plasma reactor operating at 2.45 GHz. A previously etched HPHT-grown type Ib (100)-oriented synthetic diamond was

See end of article for About the Authors.
GEMS & GEMOLOGY, Vol. 47, No. 3, pp. 202–207,
http://dx.doi.org/10.5741/GEMS.47.3.204.

used as the substrate. The growth was performed in two runs under high-power conditions (3 kW, 200 millibars, 850°C, 4% CH_4). The thickness of material deposited was 190 μm in the first growth run, and 330 μm in the second. Before deposition took place in the second run, a high-power pure hydrogen plasma was applied for 45 minutes. This step is necessary to clean and prepare the surface prior to growth. Figure 2 shows the schematics of the growth layers (left) and DiamondView images (right) taken from the cross-sectional {100} side of the sample. The HPHT-grown substrate was subsequently removed by laser cutting. After polishing, the final thickness of the sample was about 465 μm and the lateral dimensions were 4.49 × 4.52 mm.

Sample B was grown for cathodoluminescence (CL) study under similar conditions. The initial lateral dimensions before laser cutting were 4.32 × 4.32 mm. Three CVD layers were grown with thicknesses of 190, 175, and 220 μm, corresponding to two growth interruptions resulting in a final thickness of 585 μm. Before the growth was resumed, the crystal was submitted to H_2/O_2 (98%/2%) etching in high-power conditions for about 30 minutes. This ensured the surface was clean prior to growth, but it also induced a slight roughening. To access the phosphorescent region of the sample, a cross-sectional slice was prepared by laser cutting and polishing along two opposite corners. The schematics of the cross-sectional slice of sample B are illustrated in figure 3 (left). The corresponding DiamondView (center) and CL (right) images show the interfaces between the successive synthetic diamond layers.

Sample A was examined by optical microscopy combined with luminescence spectroscopy and imaging techniques. Optical micrographs were recorded using the D-Scope stereomicroscope. This microscope (with magnifications of 0.7–40×) was equipped with an illumination system consisting of darkfield, overhead daylight, and fluorescence modes. A specially designed vacuum sample manipulator allowed easy handling. Crossed-polarized images were acquired with a Leica DFC digital camera attached to a Leica DL LM microscope.

Figure 1. Colorless gem-quality CVD-grown synthetic diamonds such as these (0.22–0.31 ct) are now commercially available, making proper identification important. Photo by Robert Weldon.

Luminescence patterns generated by the intense ultra short-wave UV illumination of the DiamondView instrument were recorded with the maximum illumination power (100%), full aperture (100%), and integration times of 4–10 seconds.

Photoluminescence (PL) measurements were performed on sample A using a Renishaw inVia Raman microscope at 77 K. The system was equipped with an Ar-ion laser operating at an excitation wavelength of 514.5 nm. Highly localized PL information was acquired using a Leica Fluotar L 50× objective (NA = 0.55) in the high-confocal mode using a 2D increment of 5 μm depth × 25 μm across, with a slit width of 20 μm and a CCD area of 2 pixels (image

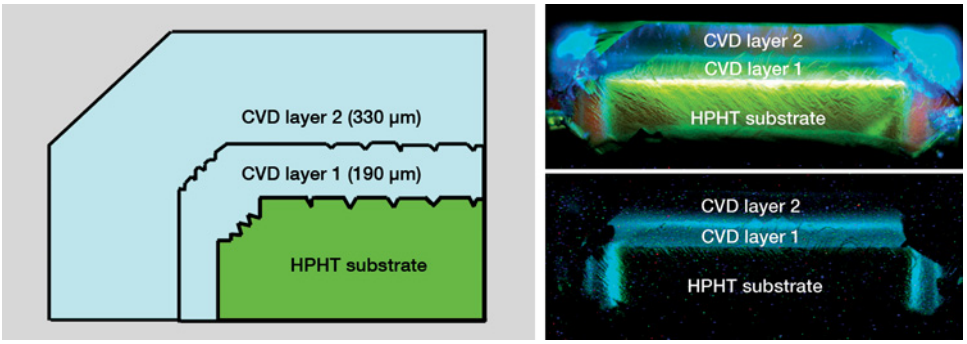

Figure 2. The schematics of the growth layers in sample A are shown for a cross-section across {100}. At right, the DiamondView luminescence (top) and phosphorescence (bottom) images show the two CVD layers and the HPHT-grown substrate.

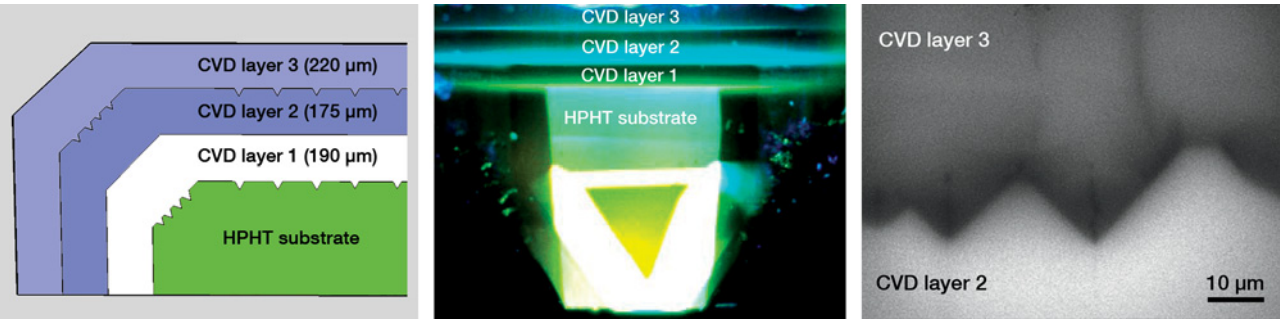

Figure 3. The schematics of the growth layers in sample B are also shown for a cross-sectional slice (across {100}, left). The DiamondView luminescence image (center) shows the successive CVD layers and the HPHT-grown substrate. The cathodoluminescence image (right) depicts the roughened interface between the CVD layers, which exhibits typical etching features and dark lines due to threading dislocations (Tallaire et al., 2011).

height) × 576 pixels (spectrometer range), resulting in an axial resolution of ~5 µm. Applying an automated xyz sample stage, we recorded detailed line and depth profiles and 2D mapping.

CL imaging of sample B was performed using a 10 kV electron beam produced in a JEOL 7001F scanning electron microscope. Monochromatic CL images were taken by filtering the excitonic signal through the monochromator, which was also equipped with a photomultiplier detector synchronized with the beam scanning.

RESULTS AND DISCUSSION

Optical Microscopy and DiamondView Imaging. Strain-related birefringence in sample A is shown in figure 4 (top left). Typical four-petal patterns related to dislocation bundles also were clearly observed. Their density was higher at the boundary with the HPHT-grown substrate, but they were also visible throughout the interior of the sample. Two examples of dislocation bundles are indicated with white arrows. Such threading dislocations in CVD synthetic diamond are usually formed at the substrate/layer interface and penetrate through the overgrowth by propagating along the [001] growth direction (Friel et al., 2009; Pinto and Jones, 2009).

The DiamondView images in figure 4 were taken from the top (growth side; upper right) and from the bottom (substrate side; lower left) of sample A, and showed a blue to blue-green "picture frame" corresponding to the interface between the subsequent CVD layers but also above the substrate imprint. In addition to the "picture frame," numerous sharp violetish blue linear features were observed; these are related to the dislocation bundles.

From the substrate side, sample A also showed a weak-to-strong red luminescence. This red luminescence originates from NV^0 and NV^- centers at 575 and 637 nm and is characteristic of trace nitrogen incorporation in this particular region of the sample. Previous measurements have shown that when no nitrogen is intentionally added to the gas phase, the nitrogen content in the synthetic diamond crystal is below 10 ppb (Tallaire et al., 2006), which is believed to be the case here. The incorporation of nitrogen impurities in the crystal was not uniform, however, since no red luminescence was observed on the other side of the sample.

NEED TO KNOW

- Production of large single-crystal CVD synthetic diamonds typically involves multiple growth runs.
- Blue to blue-green luminescent zones may be created when the growth run is interrupted and resumed.
- DiamondView, photoluminescence, and cathodoluminescence imaging were applied to study the origin and nature of these luminescent zones.
- Both silicon and boron showed preferential incorporation at the interface between CVD layers, though the exact cause of the luminescence is still under investigation.

Blue to blue-green phosphorescence lasting up to several seconds was observed (figure 4; lower right). Similar phosphorescence has been documented in HPHT-grown synthetic and treated blue type IIb diamond crystals (Watanabe et al., 1997; Lu and Eaton-Magaña, 2009). Boron-doped blue type IIb synthetic diamonds exhibit a blue to blue-green phosphores-

cence peak with a maximum at ~500 nm. In contrast, virtually all natural blue type IIb gem diamonds exhibit two phosphorescence peaks, one at ~500 nm (blue-green) and the other at ~660 nm (orange-red). In addition, it was reported that an HPHT-treated blue diamond only exhibited a peak at 500 nm (Eaton-Magana et al., 2008). These results suggest that phosphorescence spectroscopy might be an effective tool for discriminating synthetic from natural blue diamonds. In this study we report for the first time the observation of this blue to blue-green phosphorescence in (near-)colorless CVD synthetic diamond crystals where boron is present as a background impurity, as no boron was intentionally added during the growth process.

The origin of this phosphorescence has been attributed to the generally accepted donor-acceptor recombination mechanism (Dean et al., 1965), where holes bound to boron acceptors recombine with electrons that are bound to donors and emit luminescence with energy equal to the difference in energy between the donor and acceptor. The identity of the donor impurities is still under debate.

Cathodoluminescence Imaging. As shown in figure 3 (right), the interface between two successive CVD layers was clearly visible with CL imaging. The interface was slightly roughened and showed the appearance of typical etching features.

CL spectroscopy of sample B was performed in a previous study (Tallaire et al., 2011), and clearly showed the presence of boron impurities. However, it was not possible to draw conclusions about nitrogen incorporation from the CL observations.

Photoluminescence Spectroscopy and Imaging. The normalized PL emission intensity profiles of selected optical defects (NV^0 at 575.0 nm, NV^- at 637.2 nm, and a $[Si\text{-}V]^-$ doublet at 736.6–736.9 nm) on the substrate side are shown in figure 5 (right). The analyzed area is marked with an arrow in the DiamondView image in figure 5 (left). The NV luminescence decreased progressively from the edge of the layer toward the interior. The most striking feature was a sharp increase in the $[Si\text{-}V]^-$ doublet emission near the blue luminescence band. (Note: Features in the PL line scan do not reflect the strong red/orange band visible in the DiamondView image. PL measurements in the confocal mode used in this study analyze a restricted volume, and the data in figure 5 were obtained from the near-surface. Based on PL depth profile measurements [see below], there is a

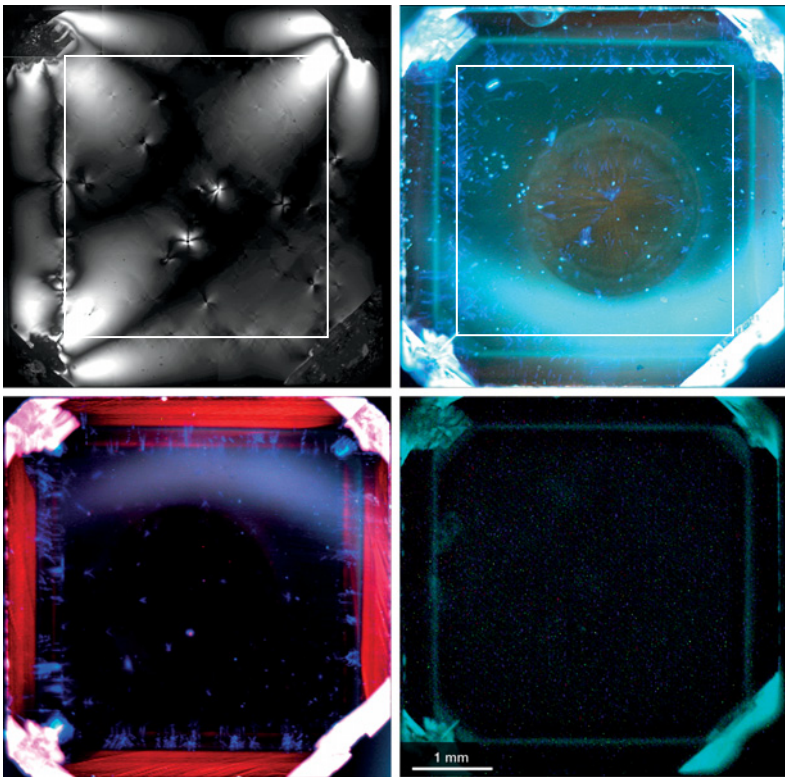

Figure 4. Strain-related birefringence (top left) was observed between crossed polarizing filters in sample A. The substrate's imprint is indicated (white square), as are two examples of dislocation bundles (arrows). In DiamondView images of the growth side (top right) and the substrate side (bottom left), a square "picture frame" corresponds to the interface between the subsequent CVD layers. The dark circular outline indicates the position of the vacuum sample manipulator. The corresponding phosphorescence image of sample A (bottom right) was recorded with a delay time of 1 millisecond. The "picture frame" is clearly presented in the phosphorescence image.

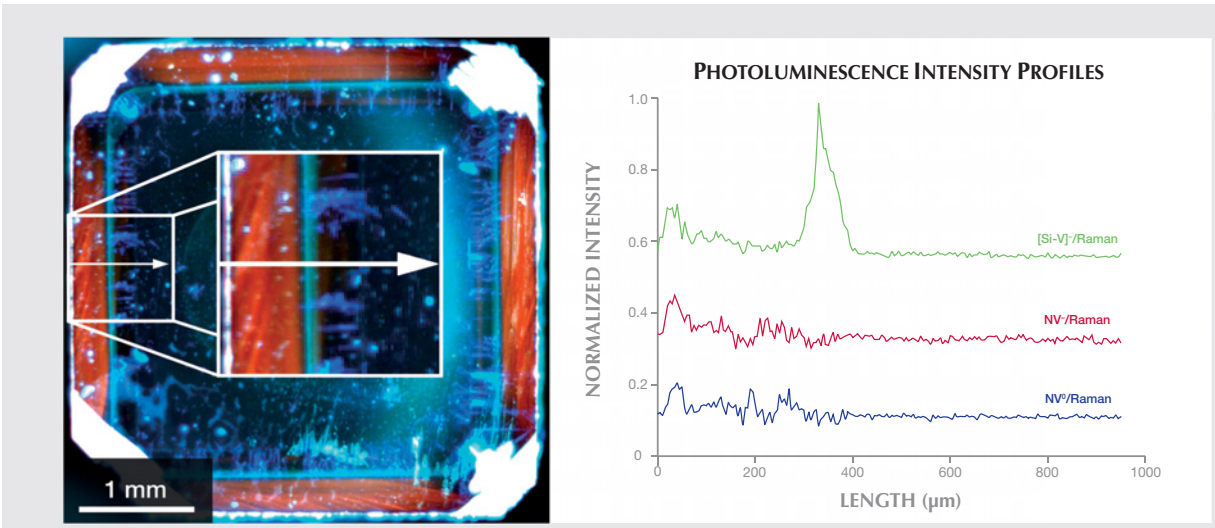

Figure 5. DiamondView imaging (left) and normalized photoluminescence intensity profiles (right) of NV^0 (575.0 nm), NV^- (637.2 nm), and $[Si\text{-}V]^-$ (736.6–736.9 nm) from the substrate side of sample A show a decrease in NV luminescence from the edge to the interior, and a sharp increase in the $[Si\text{-}V]^-$ doublet emission near the blue luminescence band.

great amount of NV luminescence centers present at depth. Also, the DiamondView image shows both fluorescence and phosphorescence; the blue to blue-green phosphorescence is much stronger and overwhelms the red-orange fluorescence.)

A combination of line and depth profiles generates 2D images reflecting the PL intensity of the diamond Raman line and the luminescence associated with the NV^0, NV^-, and $[Si\text{-}V]^-$ centers, as shown in figure 6. The $[Si\text{-}V]^-$ associated luminescence is clearly localized in a well-defined zone, and extends vertically over several tens of micrometers. Its location is consistent with the interface between the two CVD layers, suggesting preferential incorporation, as with boron. In contrast, nitrogen does not show clearly preferential incorporation.

Boron, one of the main impurities reported to cause phosphorescence, was clearly detected in both samples (see also Tallaire et al., 2011). In addition, silicon was found to be incorporated at the interrupted interface where new dislocations were formed. Although NV centers were absent, nitrogen could still be present as isolated single substitutional impurities not causing direct luminescence. The cause of the phosphorescence at the growth interruption cannot be fully determined at this time, and further studies will be required to identify the contribution of silicon, nitrogen, and dislocations.

CONCLUSIONS

Analysis using complementary luminescence spectroscopy and imaging techniques identified preferential incorporation of trace impurities in the CVD synthetic diamond crystals, especially at the interface between successive layers. CL analysis confirmed that boron is present at the interrupted inter-

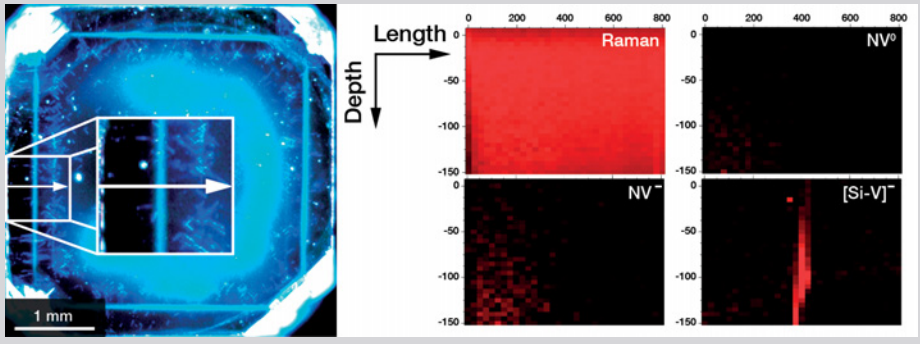

Figure 6. Photoluminescence depth profiles of the substrate side of sample B were used to create the two-dimensional maps on the right, which reflect the PL intensities of the Raman line and NV^0, NV^-, and $[Si\text{-}V]^-$ centers. The $[Si\text{-}V]^-$ luminescence is clearly localized along the interface between the two growth layers.

face, while PL showed the presence of silicon-related defects. All these impurities are present at background levels in the CVD reactor chamber. We propose that the uptake of these impurities is enhanced at the growth resumption of the crystal, leading to the appearance of a distinct luminescent pattern. On the microscopic level, the surface is roughened by the formation of etch pits that decorate threading dislocations. The surface roughening enhances the uptake of these impurities and also the generation of new threading dislocations.

The samples in this study were too thin to be cut into gemstones, but larger samples are technologically feasible. It is likely that CVD growth techniques will continue to improve, resulting in purer and larger CVD synthetic diamonds entering the gem market. The spatial distribution of spectroscopic features is important for CVD synthetic diamond identification, as they can provide evidence of the growth history and, in particular, growth interruptions that are commonly used for the synthesis of large crystals. Moreover, typical luminescence features associated with CVD synthetic diamonds (such as NV^0, NV^-, and $[Si\text{-}V]^-$), as reported in the literature (Martineau et al., 2004), were also clearly detected in this study.

The identification of CVD synthetic diamonds depends on a combination of various gemological and spectroscopic features, as no single feature will ensure proper identification. The observations obtained in this study by DiamondView, cathodoluminescence, and photoluminescence spectroscopy and imaging showed typical CVD-related optical centers. The discrete growth interruptions between subsequent CVD layers can be monitored and visualized. As such, the observations unambiguously confirmed the synthetic origin of these samples. The combination of these techniques is fully applicable in the detection and identification of natural and synthetic gem diamonds.

ABOUT THE AUTHORS

Dr. Willems (bert.willems@hrdantwerp.be) is a research scientist in the Research department of HRD Antwerp, Belgium. Dr. Tallaire is a research associate at Centre National de la Recherche Scientifique (CNRS), within the Laboratoire des Sciences des Procédés et des Matériaux (LSPM), Villetaneuse, France. Dr. Barjon is a lecturer at the Université de Versailles Saint-Quentin en Yvelines (Groupe d'Etude de la Matière Condensée, GEMaC), Meudon, France.

REFERENCES

Achard J., Tallaire A., Sussmann R., Silva F., Gicquel A. (2005) The control of growth parameters in the synthesis of high-quality single crystalline diamond by CVD. *Journal of Crystal Growth*, Vol. 284, pp. 396–405, http://dx.doi.org/10.1016/j.jcrysgro.2005.07.046.

Collins A.T. (1992) The characterization of point defects in diamond by luminescence spectroscopy. *Diamond and Related Materials*, Vol. 1, pp. 457–469, http://dx.doi.org/10.1016/0925-9635(92)90146-F.

Dean P.J., Lightowelers E.C., Wight D.R. (1965) Intrinsic and extrinsic recombination from natural and synthetic aluminum-doped diamond. *Physical Review*, Vol. 140, No. 1A, pp. A352–A368, http://dx.doi.org/10.1103/PhysRev.140.A352.

Denisenko A., Kohn E. (2005) Diamond power devices. Concepts and limits. *Diamond and Related Materials*, Vol. 14, No. 3–7, pp. 491–498, http://dx.doi.org/10.1016/j.diamond.2004.12.043.

Eaton-Magaña S., Post J.E., Heaney P.J., Freitas J., Klein P., Walters R., Butler J.E. (2008) Using phosphorescence as a fingerprint for the Hope and other blue diamonds. *Geology*, Vol. 36, pp. 83–86, http://dx.doi.org/10.1130/G24170A.1.

Friel I., Clewes S.L., Dhillon H.K., Perkins N., Twitchen D.J., Scarsbrook G.A. (2009) Control of surface and bulk crystalline quality in single crystal diamond grown by chemical vapour deposition. *Diamond and Related Materials*, Vol. 18, pp. 808–815, http://dx.doi.org/10.1016/j.diamond.2009.01.013.

Ho S.S., Yan C.S, Liu Z., Mao H.K., Hemley R.J. (2006) Prospects for large single crystal CVD diamond. *Industrial Diamond Review*, Vol. 66, pp. 28–32.

Kone S., Civrac G., Schneider H., Isoird K., Issaoui R., Achard J., Gicquel A. (2010) CVD diamond Schottky barrier diode, carrying out and characterization. *Diamond and Related Materials*, Vol. 19, pp. 792–795, http://dx.doi.org/10.1016/j.diamond.2010.01.036.

Lu R., Eaton-Magaña S. (2009) Lab Notes: Fancy Intense blue type IIb synthetic diamond. *G&G*, Vol. 45, No. 4, pp. 291–292, http://dx.doi.org/10.5741/GEMS.45.4.288.

Martineau P.M., Lawson S.L., Taylor A.J., Quinn S.J., Evans D.J.F., Crowder M.J. (2004) Identification of synthetic diamond grown using chemical vapor deposition. *G&G*, Vol. 40, No. 1, pp. 2–25, http://dx.doi.org/10.5741/GEMS.40.1.2.

Pinto H., Jones R. (2009) Theory of the birefringence due to dislocations in single crystal CVD diamond. *Journal of Physics: Condensed Matter*, Vol. 21, Art. 364220 (7 pp.), http://dx.doi.org/10.1088/0953-8984/21/36/364220.

Tallaire A., Collins A.T., Charles D., Achard J., Sussmann R., Gicquel A., Newton M.E., Edmonds A.M., Cruddace R.J. (2006) Characterisation of high-quality thick single-crystal diamond grown by CVD with a low nitrogen addition. *Diamond and Related Materials*, Vol. 15, pp. 1700–1707, http://dx.doi.org/10.1016/j.diamond.2006.02.005.

Tallaire A., Barjon J., Brinza O., Achard J., Silva F., Mille V., Issaoui R., Tardieu A., Gicquel A. (2011) Dislocations and impurities from etch-pits at the epitaxial growth resumption of diamond. *Diamond and Related Materials*, Vol. 20, pp. 875–881, http://dx.doi.org/10.1016/j.diamond.2011.04.015.

Walker J. (1979) Optical absorption and luminescence in diamond. *Reports of Progress in Physics*, Vol. 42, pp. 1605–1659, http://dx.doi.org/10.1088/0034-4885/42/10/001.

Watanabe K., Lawson S.C., Isoya J., Kanda H., Sato Y. (1997) Phosphorescence in high-pressure synthetic diamond. *Diamond and Related Materials*, Vol. 6, pp. 99–106, http://dx.doi.org/10.1016/S0925-9635(96)00764-9.